Computational and Structural Biotechnology Journal 21 (2023) 2759–2766

Contents lists available at ScienceDirect

Computational and Structural Biotechnology Journal

journal homepage: www.elsevier.com/locate/csbj

Discovery of a highly efficient TylF methyltransferase via random mutagenesis for improving tylosin production

Jingyan Fan [a], Zhiming Yao [a], Chaoyue Yan [a], Meilin Hao [a], Jun Dai [a,d,e], Wenjin Zou [a], Minghui Ni [a], Tingting Li [a], Lu Li [a,b,c], Shuo Li [d,e], Jie Liu [d,e], Qi Huang [a,b,c,*], Rui Zhou [a,b,c,e,*]

[a] National Key Laboratory of Agricultural Microbiology, College of Veterinary Medicine, Huazhong Agricultural University, Wuhan 430070, China
[b] International Research Center for Animal Disease (Ministry of Science and Technology of China), Wuhan 430070, China
[c] Cooperative Innovation Center of Sustainable Pig Production, Wuhan 430070, China
[d] Hubei Provincial Bioengineering Technology Research Center for Animal Health Products, Yingcheng 432400, China
[e] The HZAU-HVSEN Research Institute, Wuhan 430042, China

ARTICLE INFO

Article history:
Received 22 December 2022
Received in revised form 11 April 2023
Accepted 11 April 2023
Available online 20 April 2023

Keywords:
Streptomyces fradiae
Tylosin
Rate-limiting enzyme
Macrocin *O*-methyltransferase
Catalytic activity
Directed protein evolution

ABSTRACT

Macrolides are currently a class of extensively used antibiotics in human and animal medicine. Tylosin is not only one of the most important veterinary macrolides but also an indispensable material for the bio- and chemo-synthesis of new generations of macrolide antibiotics. Thus, improving its production yield is of great value. As the key rate-limiting enzyme catalyzing the terminal step of tylosin biosynthesis in *Streptomyces fradiae* (*S. fradiae*), TylF methyltransferase's catalytic activity directly affects tylosin yield. In this study, a *tylF* mutant library of *S. fradiae* SF-3 was constructed based on error-prone PCR technology. After two steps of screening in 24-well plates and conical flask fermentation and enzyme activity assay, a mutant strain was identified with higher TylF activity and tylosin yield. The mutation of tyrosine to phenylalanine is localized at the 139th amino acid residue on TylF ($TylF^{Y139F}$), and protein structure simulations demonstrated that this mutation changed the protein structure of TylF. Compared with wild-type protein TylF, $TylF^{Y139F}$ exhibited higher enzymatic activity and thermostability. More importantly, the Y139 residue in TylF is a previously unidentified position required for TylF activity and tylosin production in *S. fradiae*, indicating the further potential to engineer the enzyme. These findings provide helpful information for the directed molecular evolution of this important enzyme and the genetic modification of tylosin-producing bacteria.

1. Introduction

Macrolides are a group of antibiotics extensively used in human and animal medicine. Tylosin, as the first generation of veterinary macrolide antibiotic introduced in 1961, is still one of the most commonly used antibiotics in livestock and other animals [1]. It is mainly used in the clinical treatment of animal infections caused by Gram-positive bacteria and mycoplasma, and was also once served as a growth promoter for pigs and poultry [2,3]. More importantly, tylosin is an indispensable material for the bio- or chemo-synthesis of new generations of macrolide antibiotics such as timicosin, tylvalosin, tildipirosin, and tulathromycin [4–7]. It also functions as a basic compound for developing novel antibiotics by structural derivation as well [8].

Tylosin is comprised of 16-membered tylactone and three deoxyhexose sugars, and can be produced by *Streptomyces fradiae* (*S. fradiae*) [1], *Streptomyces rimosus* [9], and *Streptomyces hygroscopicus* [10]. *S. fradiae* is the most common tylosin industrial producer, and improving the productivity of the industrial producers is critical for antibiotics industry. Currently, the main strategies for breeding superior strains include traditional mutagenesis and genetic engineering approaches. However, with the development of molecular

Abbreviations: aa, amino acid; HPLC, high-performance liquid chromatography; IPTG, isopropyl-β-D-thiogalactopyranoside; *S. fradiae*, *Streptomyces fradiae*; KD, equilibrium dissociation constant; LB, lysogeny broth; MTP, microtiter plate; PMSF, phenylmethanesulfonyl fluoride; RU, resonance unit; SAH, S-adenosyl-L-homocysteine; SAM, S-adenosyl-L-methionine; SPR, surface plasmon resonance; TSA, tryptic soy agar; TSB, tryptic soy broth

* Correspondence to: College of Veterinary Medicine, Huazhong Agricultural University, Wuhan 430070, China.
E-mail addresses: qhuang@mail.hzau.edu.cn (Q. Huang), rzhou@mail.hzau.edu.cn (R. Zhou).

https://doi.org/10.1016/j.csbj.2023.04.005

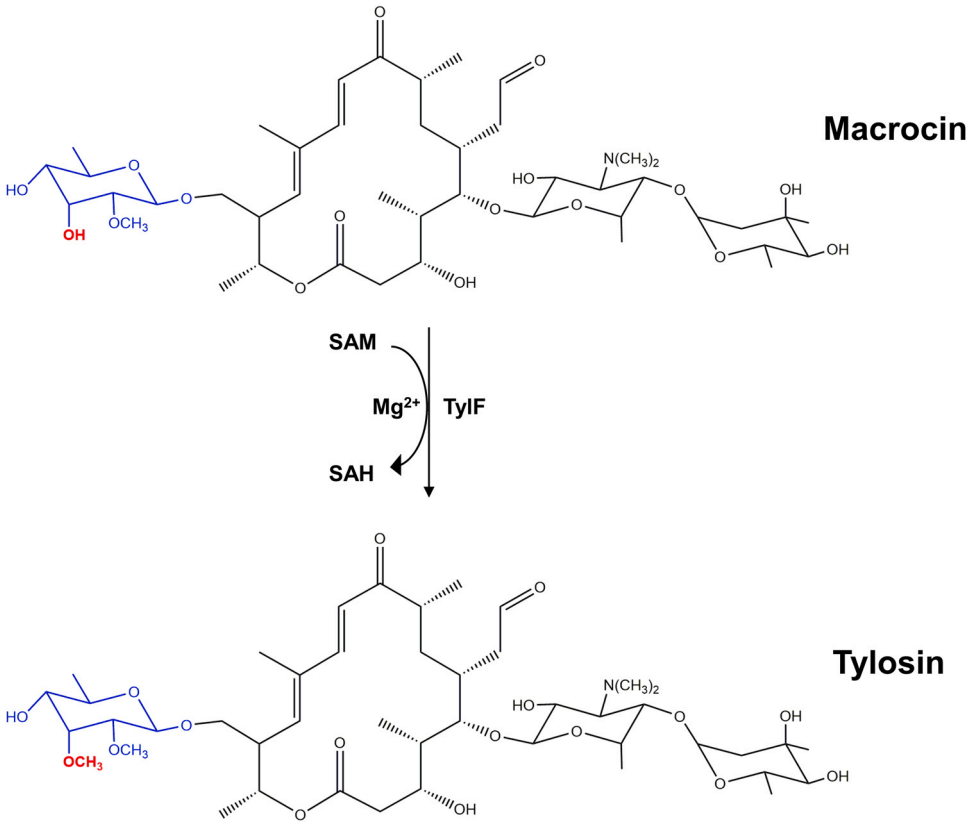

Fig. 1. Reaction catalyzed by macrocin *O*-methyltransferase TylF to convert macrocin to tylosin.

biology and synthetic biology, targeted-genetic engineering is a more accurate and efficient approach with broad prospects in developing high-yield producers.

The tylosin biosynthetic gene cluster in *S. fradiae* has been validated and sequenced, and its biosynthetic pathway was identified [11–13]. Tylactone, the cyclized polyketide product, was first synthesized, and then glycosylated by stepwise adding mycaminose, deoxyallose, and mycarose to generate demethyl-macrocin. Then the bis *O*-methylation gradually converts the deoxyallose to mycinose, producing tylosin C (also known as macrocin) and converting it to tylosin A (usually called tylosin) [14]. TylF, a S-adenosyl-L-methionine (SAM)-dependent *O*-methyltransferase, catalyzes the conversion of macrocin to tylosin (Fig. 1) that is the terminal and major rate-limiting step in the tylosin biosynthesis pathway of *S. fradiae* [15]. Several studies have revealed that TylF is closely related to the yield of tylosin, and the high tylosin yield is usually accompanied with the high catalytic activity of TylF [16–18]. During fermentation, the enzyme activity of TylF reaches the maximum at about 72 h and then decreases slowly. The low enzyme activity of TylF during the fermentation will lead to a high content of macrocin that is difficult to be removed from the final product tylosin. Therefore, developing highly efficient TylF methyltransferase is crucial to achieve high tylosin production.

As an indispensable biocatalyst, although enzymes have higher catalytic efficiency compared with chemical catalysts in biochemical reactions, natural enzymes require improved enzyme stability, substrate specificity, and environmental compatibility to meet the requirements of biochemical reactions, especially in industrial processes [19]. Directed evolution, a successful protein engineering technology to enhance or alter the activity of biomolecules, mimics the process of natural evolution, but on a much-shortened timescale [20,21]. The general strategies of directed evolution mainly include gene diversification, gene expression, and screening. Genetic diversity is achieved commonly through error-prone PCR [22], DNA shuffling [23], cassette mutagenesis [24], *etc*., and then improved enzyme variants are screened and selected [20]. This technology is increasingly being used in industrial processes, research, and other therapeutic application. Error-prone PCR works by reducing the fidelity of the Taq enzyme via changing the PCR reaction conditions so that the base mismatch in the product occurs with a certain probability to fulfill the needs of directed evolution, which is time-saving and of high efficiency.

In this study, we first constructed a *tylF* deletion strain of *S. fradiae*. By using error-prone PCR, a mutagenesis library of *tylF* was constructed which was complemented to the Δ*tylF* strain to screen mutant strains with higher tylosin yield. Nine mutants with increased production of tylosin were identified. Among them, a novel TylF variant TylF^{Y139F} was confirmed and further characterized. This amino acid substitution altered the protein structure and increased catalytic activity of TylF enzyme for the conversion of macrocin to tylosin.

2. Materials and methods

2.1. Bacterial strains, culture conditions, and plasmids

The bacterial strains and plasmids used in this work are shown in Table S1. *S. fradiae* SF-3, an industrial strain, donated by HVSEN Biotech Co., Ltd, Wuhan, China, was used for the construction of the *tylF*-mutant library. Plasmids pKC1139 and pSET152 [25] were used to construct deletion and expression strains, respectively. *S. fradiae* strains were cultured in tryptic soy broth (TSB) or on tryptic soy agar (TSA) (BD, Franklin Lakes, NJ, USA) and Gause's No.1 medium containing 10 g KNO_3, 1 g NaCl, 0.8 g $K_2HPO_4{\cdot}3\,H_2O$, 0.5 g $MgSO_4{\cdot}7\,H_2O$, 0.01 g $FeSO_4{\cdot}H_2O$, 20 g agar, and 20 g corn starch per liter (pH 7.2) at 30 °C. Apramycin (50 μg/ml) was used to screen the transformants

and complementary strains. *E. coli* DH5α was served as the host strain for regular cloning, and *E. coli* BL21(DE3) was used for prokayotic expression of His-tag fusion proteins. *E. coli* ET12567 was used for *E. coli-Streptomyces* conjugal transfer, and was cultivated with chloramphenicol (25 μg/ml) and kanamycin (25 μg/ml). *E. coli* were grown in lysogeny broth (LB) or on LB agar at 30 °C.

The seed medium and the fermentation medium were used for the fermentation of the *Streptomyces* strains. The seed medium contained (per liter) 5 g yeast extract powder, 5 g soybean cake flour, 6 g corn steep liquor, 3 g $CaCO_3$, and 5 g soybean oil (pH 7.2). The fermentation medium contained (per liter) 41.4 g soybean oil, 8 g corn gluten flour, 2 g cottonseed meal, 14 g corn flour, 7 g fish meal, 5 g hot fried soybean cake flour, 4 g peanut meal, 0.9 g betaine hydrochloride, 6 mg $CoCl_2{\cdot}6\,H_2O$, 0.3 g $MgSO_4{\cdot}7\,H_2O$, 4 mg $NiSO_4{\cdot}6\,H_2O$, 0.1 g $(NH_4)_2HPO_4$, and 2 g $CaCO_3$ (pH 7.0).

2.2. Construction of tylF deletion mutant and complemented strain

To obtain *tylF* deletion mutant, the up- and down-stream fragments flanking *tylF* were amplified from the *S. fradiae* SF-3 genome DNA with primers Δ*tylF*-A/Δ*tylF*-B and Δ*tylF*-C/Δ*tylF*-D (Supplementary Table S1) according to published sequence information (GenBank accession number AF147703.1), and were ligated into the shuttle vector pKC1139. The recombinant plasmid was electroporated into the donor strain *E. coli* ET12567 and then introduced into *S. fradiae* SF-3 via *E. coli-Streptomyces* conjugative transfer. Subsequently, the isogenic deletion strain was achieved through double homologous recombination as described previously with modification [26].

For complemented strain construction, the fragment containing the promoter and coding sequence region of *tylF* was amplified with primers CΔ*tylF*-F/CΔ*tylF*-R (Supplementary Table S1), and ligated into pSET152 vector. The recombinant plasmid pSET152:*tylF* was introduced into Δ*tylF* to generate the complemented strain CΔ*tylF*. *tylF* and its up- and down-stream genes were verified by PCR analysis with primers *tylF*-F/*tylF*-R, *tylJ*-F/*tylJ*-R and *tylH1*-F/*tylH1*-R (Supplementary Table S1).

2.3. Concentration determination of tylosin and other intermediates

To determine tylosin production, the strains were first cultured in conical flasks containing 50 ml seed medium at 30 °C with rotary shaking at 220 rpm for 2 days to obtain mycelium, and then the mycelium was sub-cultured in 30 ml of fermentation medium for another 7 days under the same conditions. The fermentation products were extracted through centrifugation and the tylosin was quantified by Agilent 1260 series high-performance liquid chromatography (HPLC) (Agilent Technologies, Palo Alto, CA, USA) using a C18 column (ODS-3, 4.6 × 250 mm, Φ 5 μm) as previously described [27]. The column temperature was maintained at 30 °C. The mobile phase consisted of 2 M sodium perchlorate (pH 2.5) and acetonitrile at 60: 40 (v/v), and the eluate (flow rate of 1.0 ml/min) was monitored by absorbance at 280 nm.

2.4. Construction of tylF gene mutant library

Random mutations were introduced into DNA fragments through error-prone PCR technique. The error-prone PCR was performed in 50 μL buffer (total volume) containing 1 × Taq buffer, 4 mM $MgCl_2$, 0.2 mM dATP, 0.2 mM dGTP, 1 mM dTTP, 1 mM dCTP, 0.4 μM each primer *tylF*-F_{pF}/*tylF*-$R_{152\,N}$, 0.1–0.3 mM $MnCl_2$, 20 ng template DNA, and 5 U Taq DNA Polymerase (Cwbio, Taizhou, China), using a PCR program: 94 °C for 5 min; 30 cycles at 94 °C for 30 s, 58 °C for 30 s, and 72 °C for 45 s; and finally at 72 °C for 3 min. The PCR product was purified with E.Z.N.A.® Cycle-Pure Kit (Omega, Norcross, GA, USA).

The promoter of gene *tylF* was amplified with primers p*tylF*-F_{152}/p*tylF*-R_F, and was cloned into pSET152 together with the the mutation-containing *tylF* fragments via seamless cloning. Subsequently, the recombinant plasmids pSET152: ep-*tylF* that carrying diverse *tylF* fragments were transferred into *E. coli* DH5α cells to prepare the plasmid library. Then, the plasmid was electroporated into *E. coli* ET12567, which was used as the donor to deliver the mutated *tylF* into the Δ*tylF* strain through *E. coli-Streptomyces* conjugal transfer and integration of the plasmids into the phage attachment site *attB* of the Δ*tylF* strain genome.

2.5. High-through screening of mutant library

High-through screening was performed as previously described with some modifications [28]. The mutants were precultured with 2 ml seed medium per well in 24-well deep microtiter plates (MTPs) for 2 days, then subcultured in 1.5 ml fermentation medium at 10% (v/v) for another 5 days. The other culture conditions were the same as shake flasks, and the fermentation products were measured as above.

2.6. Monitoring the conversion of macrocin to tylosin during fermentation

The fermentation of high-yield mutants was performed in conical flasks. The products of fermentation were extracted at five time points within 7 days (2, 4, 6, 6.5, and 7 days), and the contents of macrocin and tylosin were analyzed with HPLC as described above. The mutation sites in *tylF* in the high-yield strains were determined by sequencing the PCR products with primers *tylF*-F_{pF}/*tylF*-$R_{152\,N}$.

2.7. Protein expression and purification

To express the protein TylF and $TylF^{Y139F}$, the coding sequences of gene *tylF* and $tylF^{Y139F}$ were amplified respectively from the genome DNA of wild strain SF-3 and the mutant EP11–6, and ligated into pET28a to obtain recombinant plasmids pET28a-*tylF* and pET28a-$tylF^{Y139F}$ in *E.coli* DH5α cells [29]. The recombinant plasmids were then transformed into *E. coli* BL21 (DE3) cells for the expression of N-terminal His_6-tagged TylF and $TylF^{Y139F}$. The transformants were cultivated at 37 °C in LB with kanamycin (25 μg/ml) for 3–4 h until OD_{600} reached 0.6–0.8, and protein expression was induced by adding 0.1 mM isopropyl-β-D-thiogalactopyranoside (IPTG) and incubating overnight at 18 °C. The cultures were centrifuged at 10,000 r/min for 15 min to harvest the cells, and the cell pellets were resuspended in lysis buffer (50 mM Tris-HCl, 300 mM NaCl, 20 mM imidazole, 10%(v/v) glycerol, pH 7.6) and lysed under a high-pressure cell crusher (Life Technologies, Carlsbad, CA, USA). His_6-tagged TylF and $TylF^{Y139F}$ were purified using Ni-NTA columns (GE Healthcare, Piscataway, NJ, USA), and the whole processes were carried out at 4 °C. Bound His_6-tagged proteins were eluted with elution buffer (50 mM Tris-HCl, 300 mM NaCl, 500 mM imidazole, 10% (v/v) glycerol, pH 7.6) and further purified and concentrated using 10 kDa size-exclusion filters (Millipore, Boston, MA, USA). The final desalting step is buffer exchange into storage buffer (50 mM Tris-HCl, 10%(v/v) glycerol, pH7.6), and the purified proteins were detected by SDS-PAGE.

2.8. Enzyme assays

Enzyme activity assays were carried out as described previously with some modifications [30]. The optimized enzyme reaction was conducted in 1 ml reaction buffer (50 mM Tris-HCl, 10 mM $MgCl_2$, 1 mM phenylmethanesulfonyl fluoride (PMSF), 6 mM 2-mercaptoethanol, pH 7.6), and initiated by adding protein, SAM (0.4 mM final), and macrocin (0.2 mM final). After incubation at 30 °C for 1 h, the reaction mixture was terminated by incubation with boiling

water for 10 min, and the supernatant was collected by centrifugation for HPLC analysis.

2.9. Protein structural prediction

The structures of TylF and TylF^{Y139F} proteins were modeled using the I-TASSER server (http://zhanglab.ccmb.med.umich.edu/I-TASSER) [31,32], and the models (stereoviews) of TylF and TylF^{Y139F} were visualized using PyMOL (version 2.0.6.0).

2.10. Binding affinity measurement by surface plasmon resonance (SPR)

The binding affinity of the TylF (TylF^{Y139F}) proteins with the SAM were detected using the OpenSPR system (Nicoya Lifesciences, ON, CA). Proteins were separately fixed on the NTA sensor chips (Cat#SEN-AU-100–10-NTA; Nicoya Lifesciences, ON, CA). The sensor chips were first activated with a mixture of imidazole and $NiCl_2$ solution, and then the TylF or TylF^{Y139F} protein was diluted with immobilization buffer (50 mM Tris-HCl, 10 mM $MgCl_2$, pH=7.6) and injected into chips at a flow rate of 20 μL/min for 240 s to reach a capture level. Subsequently, SAM was diluted to different concentrations (50, 100, 200, 400, and 800 μM) with the running buffer (50 mM Tris-HCl, 10 mM $MgCl_2$, pH=7.6), and was injected to flow cell of channel at a flow rate of 20 μL/min for an association of 240 s at 25 °C in the running buffer, followed by 240 s dissociation. After each cycle of interaction analysis, the chips were regenerated with 350 mM EDTA at a flow rate of 30 μL/min. The data were analyzed by the one-to-one analysis model using TraceDrawer software (Ridgeview Instruments ab, Sweden).

3. Results

3.1. Construction of tylF deletion mutant and complemented strain

A knockout mutant of *tylF* (Δ*tylF*) and its complemented strain CΔ*tylF* of *S. fradiae* strain SF-3 were constructed and verified by PCR amplification, fermentation, and tylosin determination (Supplementary Fig. S1). The HPLC results of fermentation demonstrated that the *tylF* knockout completely blocked the conversion from macrocin to tylosin, and the complementation of *tylF* expression restored the production of tylosin (Supplementary Fig. S1). This confirms that *tylF* is an indispensable component in tylosin biosynthesis and suggests that the complementation of *tylF* was achieved.

3.2. Generation and evaluation of a tylF gene mutant library

In order to construct a *tylF* gene mutant library in SF-3, we complemented *tylF* with random mutations to the Δ*tylF* strain. By using error-prone PCR, the *tylF* coding sequence with random mutations were obtained and then cloned into pSET152 vector, and the resulting recombinant plasmids pool was transformed into *E. coli* DH5α cells. By sequencing the plasmids extracted from the transformants, base mismatches in the error-prone PCR products were determined to be approximately 90–100%. A mutant library was then obtained by mixing all the transformants which consisted of approximately 1×10^5 clones. Subsequently, the recombinant plasmids extracted from the library were introduced into the Δ*tylF* strain, and the transformants were selected using apramycin (50 μg/ml) and nalidixic acid (25 μg/ml) and subjected to screening for mutant strains with higher tylosin yield (Fig. 2).

3.3. Screening of the high-yield strains

In the first-round screening, 500 mutants were assayed using a high-throughput assay in 24-well plates for fermentation. A total of 15 mutant strains showed higher tylosin production than the strains SF-3 and CΔ*tylF* according to the HPLC determination (Fig. 3A). Subsequently, all the 15 mutants were fermented in 250 ml conical flasks to further determine the yield, and nine mutants exhibited a higher yield of tylosin (Fig. 3B).

As TylF catalyzes the conversion of macrocin to tylosin, we next determined the content of these two products in the fermentation supernatants of these nine mutant strains. It was revealed that the yield of tylosin in all mutants was higher than that in the strains SF-3 and CΔ*tylF* from the fourth day (Fig. 3C). Meanwhile, the macrocin of most mutants almost disappeared or was at a lower level in the late stage of fermentation, while accumulation of macrocin was observed for strains SF-3 and CΔ*tylF* from the second day of fermentation (Fig. 3D). These results suggested that all nine mutants have a higher conversion efficiency of macrocin to tylosin, indicating that these mutants may possess more efficient TylF enzymes.

3.4. Mapping the mutation sites of tylF gene in high-yield mutants

By amplifying the *tylF* gene from the genome of the mutant strains and DNA sequencing analysis, the mutation sites in *tylF* gene of the high-yield mutants were identified. As shown in Table 1, sense mutations were identified in all nine mutants, and the number of amino acid mutation per protein varied from 1 to 3. Notably, the Y139F mutation occurred in both EP11–6 and EP11–10 strains, indicating a possible critical role of this point mutation which was selected for further investigation.

3.5. Increased catalytic activity and tolerance to temperature of TylF^{Y139F}

To investigate whether the Y139F mutation of TylF influences its catalytic activity, His_6-tagged TylF and TylF^{Y139F} were purified from recombinant *E. coli* (Fig. 4A). Under certain conditions, the in vitro enzymatic activities of TylF and TylF^{Y139F} were determined, and the results revealed that the mutant protein TylF^{Y139F} exhibited an elevated macrocin *O*-methyltransferase activity compared with wild-type TylF (Fig. 4B). Moreover, TylF^{Y139F} was more resistant to temperature shift as the TylF^{Y139F} variant had a high activity between 28 °C and 40 °C, while the wild-type TylF reached the high activity only at 34–40 °C (Fig. 4C).

3.6. Altered three-dimensional structure of TylF^{Y139F} protein

The structural modeling of TylF and TylF^{Y139F} proteins were performed using I-TASSER and visualized using PyMOL as shown in Fig. 5. It was displayed that TylF (Fig. 5A) and TylF^{Y139F} (Fig. 5B) showed two different conformations. The yellow marked region (residues 133 −143) at the top of TylF showed an α-helix while it became a random coil in TylF^{Y139F}. The random coil of the blue marked region (residues 82 −86) in the TylF formed a β-sheet in the TylF^{Y139F}. In addition, the disappearance of the α-helix in the yellow-marked region of the TylF^{Y139F} protein directly led to the remarkably enlarged entrance for the cavity near this region compared to TylF (Fig. 5C and 5D).

3.7. Reduced SAM binding stability of TylF^{Y139F}

In order to further investigate whether the change of the protein structure of TylF^{Y139F} influences its binding to the SAM, the binding affinity of the TylF (TylF^{Y139F}) proteins with the SAM were detected by SPR. The SPR results demonstrated that the resonance units (RUs) of both TylF and TylF^{Y139F} were significantly responsive to SAM at different concentrations, and the calculated binding affinity of SAM with TylF (equilibrium dissociation constant (KD)= 162 ± 91.6 μM) was found to be higher than that of TylF^{Y139F} (KD=265 ± 24.3 μM) (Fig. 6A and 6B), indicating a decreased SAM binding stability of TylF^{Y139F}.

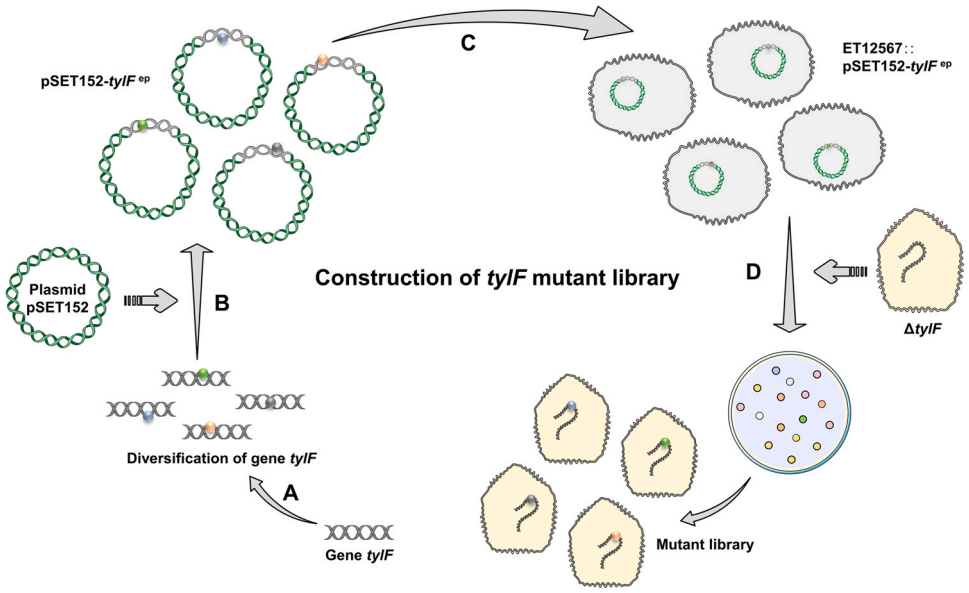

Fig. 2. Schematic diagram of *tylF* gene mutant library construction. (A) Introducing random mutations into *tylF* by error-prone PCR. (B) Construction of recombinant plasmids pSET152: ep-*tylF* through seamless cloning in *E. coli* DH5α. (C) The recombinant plasmids were electroporated into recipient bacteria *E. coli* ET12567. (D) Mutant Δ*tylF* acquired the genetic diversification ep-*tylF* through the *E. coli-Streptomyces* conjugal transfer.

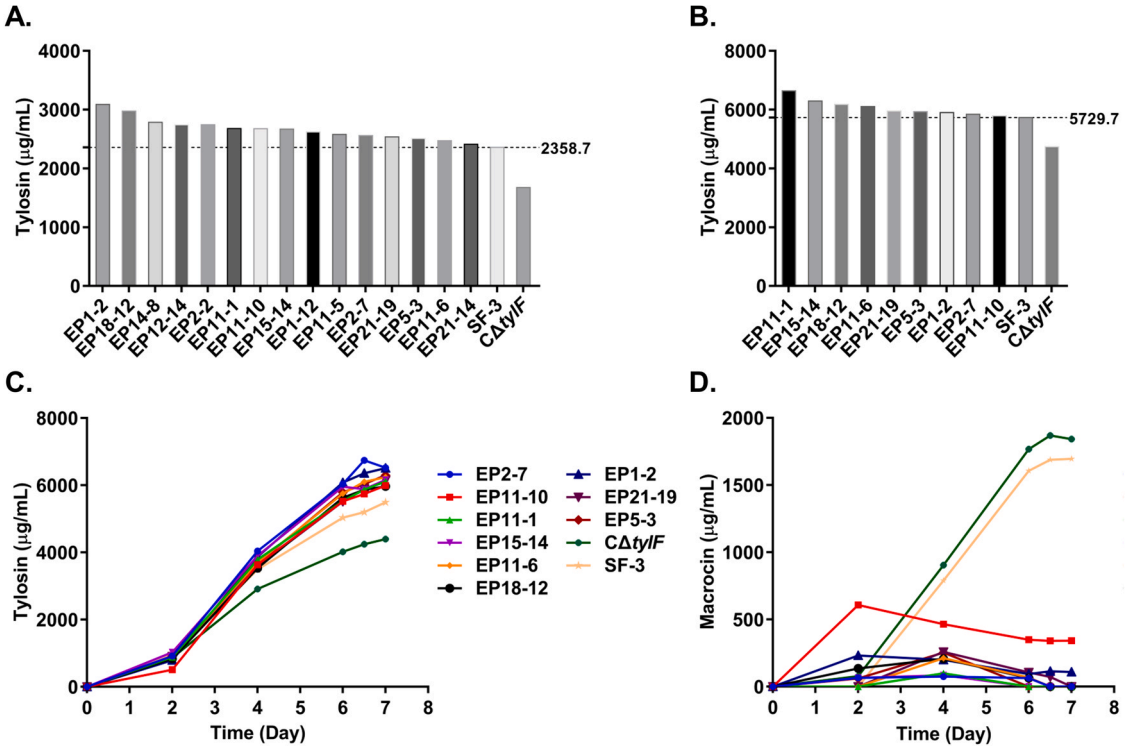

Fig. 3. Screening of high-yield strains. (A) Determination of tylosin production for the high-yield mutatant strains. The indicated *Streptomyces* strains were cultured in 24-deep-well MTPs, and the products were analyzed by HPLC. (B) Further verification of tylosin yield in conical flask. The fermentation of the high-yield strains were performed in conical flask, and the products were analyzed by HPLC. (C) and (D) Quantification of tylosin and macrocin in the fermentation products. The fermentation products of the high-yield strains were analyzed by HPLC at five time points within 7 days (2, 4, 6, 6.5, 7 days), and content curves of tylosin and macrocin were displayed.

4. Discussion

Macrolide antibiotics are a class of antibiotics widely used in human and animals. Tylosin, as a first-generation veterinary macrolide antibiotic, is also an indispensable material for the bio- and chemo-synthesis of new generations of macrolide antibiotics, therefore improving its production yield is of great importance.

S. fradiae is the most common tylosin industrial producer, and the current breeding of tylosin superior strains is highly dependent on chemical or/and physical random mutagenesis such as low-dose UV and 5-bromouracil, *etc*. Khaliq et al. treated *S. fradiae* strain NRRL-2702 using UV or/and γ-rays and obtained strains with 3 times and 5 times higher tylosin yield than the original strain, respectively [33]. Although these traditional mutagenesis approaches have achieved positive progress in the past decades, it becomes more and more difficult to obtain

Table 1
Mutation sites of gene *tylF* in high-yield strains.

Mutant strain	Number of amino acid mutation	Mutation and its position
EP1–2	2	aa25: TAC-CAC; aa256: GGC-GAC
EP2–7	2	aa138: CAG-CAT; aa232: TTC-TAC
EP5–3	2	aa48: GGC-GGT; aa62: AAG-GAG
EP11–1	2	aa36: ACC-CCC; aa54: GTC-GCC
EP11–6	1	aa139: TAC-TTC
EP11–10	1	aa139: TAC-TTC
EP15–14	3	aa123: CTG-CCG; aa165: AAC-AGC; aa182: GTG-GCG
EP18–12	1	aa197: GCC-ACC
EP21–19	1	aa54: GTC-GAC

aa: amino acid

new high-yield strains due to randomness, invalidity, and negativity of mutation. Therefore, targeted-genetic engineering is a more accurate and purposeful approach for developing high-yield producers.

Based on the principle of natural evolution, researchers modify protein properties, increase catalytic activity, or create novel protein catalysts through multiple mutagenesis and screening for use in industrial processes to manufacture chemicals, pharmaceuticals, and materials for human society [34]. As a time-saving, effective, and powerful technique, the directed evolution of protein has been extensively used and made remarkable progress in the industrial application of biocatalysis. For instance, in *Bacillus subtilis*, the endo-beta-1,4-glucanase (Cel5A) hydrolyzes cellulose by cleavage of the internal bonds in the glucose chains, producing new ends randomly. Lin et al. evolved several Cel5A variants with improved catalytic activity toward sodium carboxymethyl cellulose grounded on error-prone PCR and DNA shuffling [35]. Moreover, based on the random-priming recombination (RPR) method, a new thermostable variant subtilisin E was developed by Shao and colleagues via the mutagenesis and recombination of RC1 and RC2 genes encoding thermostable subtilisin E variants [36]. Thus, the directed evolution of related important proteins in the synthesis of tylosin also has great practical significance for breeding high-yield strains.

So far, the macrocin *O*-methyltransferase TylF is the only rate-limiting enzyme discovered in tylosin synthesis pathway, which is essential for the efficient production of tylosin. However, the enzyme activity of TylF can not maintain a sustained high level during the whole fermentation process, but only reaches the maximum at about 72 h and then gradually goes down by negative feedback regulation [16]. Accordingly, it is quite necessary to maintain the high catalytic activity of TylF enzyme during fermentation. In this study, a screening platform was established for macrocin *O*-methyltransferase evolution. After two steps of screening, 24-well plate screening and further verification in conical flasks, nine mutants involving TylF mutations and increased tylosin production were validated. Furthermore, all nine mutants have a higher conversion efficiency of microcin to tylosin, which significantly reduced the accumulation of macrocin during fermentation. To search for an efficient TylF among the nine mutants, the mutated protein TylF^{Y139F} in the mutant strains EP11–6 and EP11–10 was further confirmed. *In vitro* enzyme activity assays demonstrated that, compared with TylF, TylF^{Y139F} exhibited remarkably higher catalytic efficiency to the conversion of

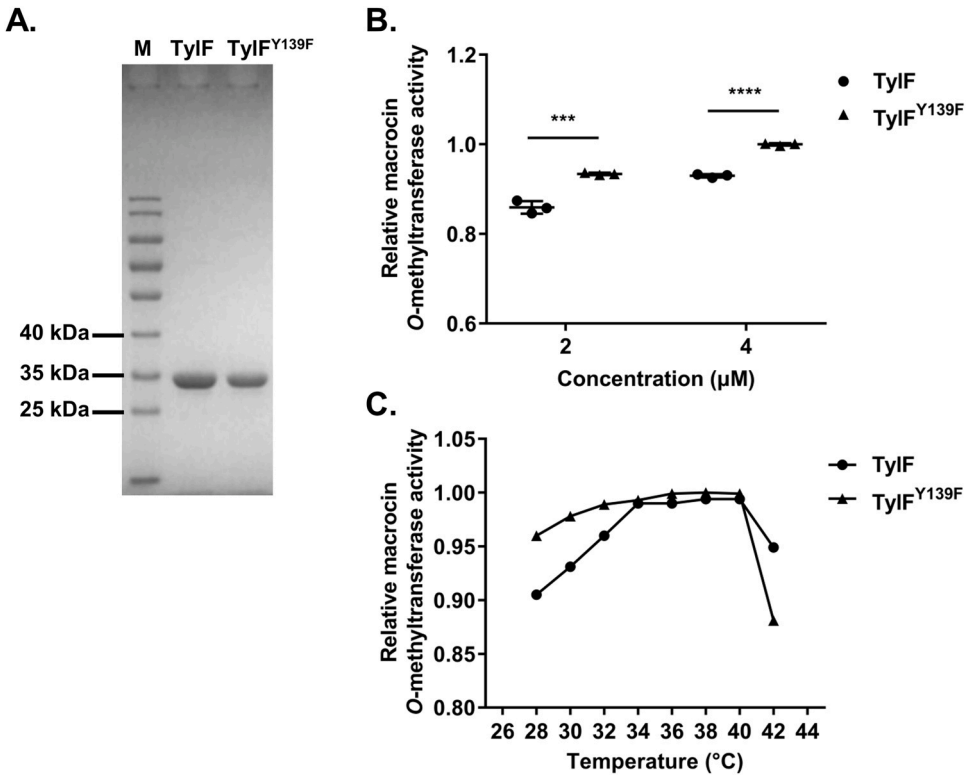

Fig. 4. Enzyme activity analysis of TylF and TylF^{Y139F}. (A) SDS-PAGE analysis. (B) and (C) Relative macrocin O-methyltransferase activity assays. Enzyme activity assays of TylF and TylF^{Y139F} were performed with different concentration of enzymes (B) or at different termperature (C). The reaction products were analyzed by HPLC. Statistical significances were determined by using the Student's t-test. * ** indicates $p < 0.001$, and * *** indicates $p < 0.0001$.

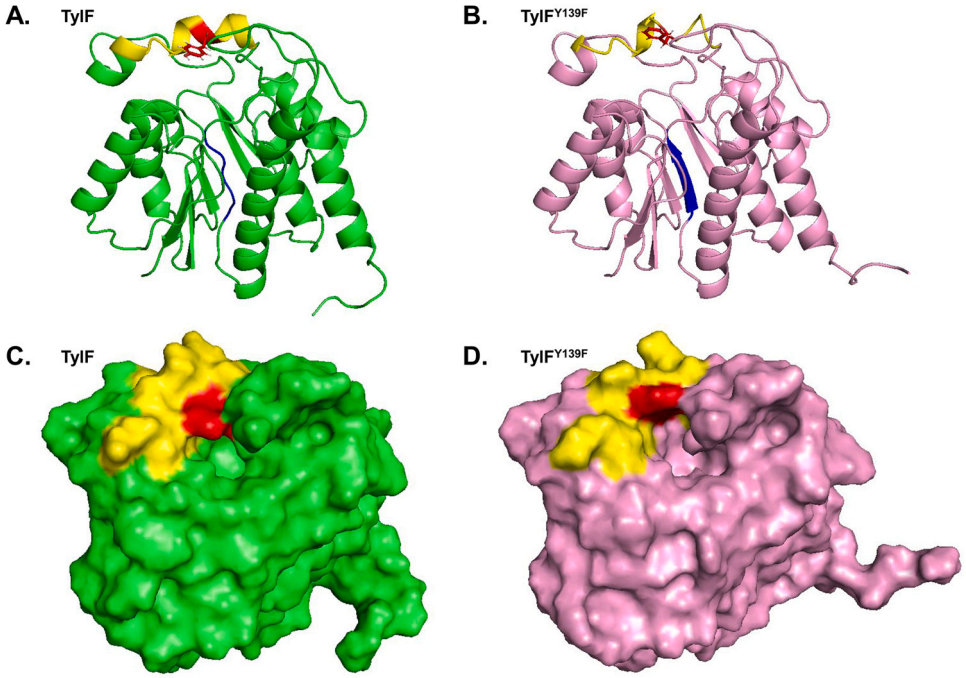

Fig. 5. Stereoviews showing the overall structure of TylF and TylF^{Y139F}. (A) and (B) Cartoon representation. (C) and (D) Molecular surface representation. Throughout, the mutation site is colored red. Different regions between TylF and TylF^{Y139F} were shown in blue (residues 82–86) and yellow (residues 133–143).

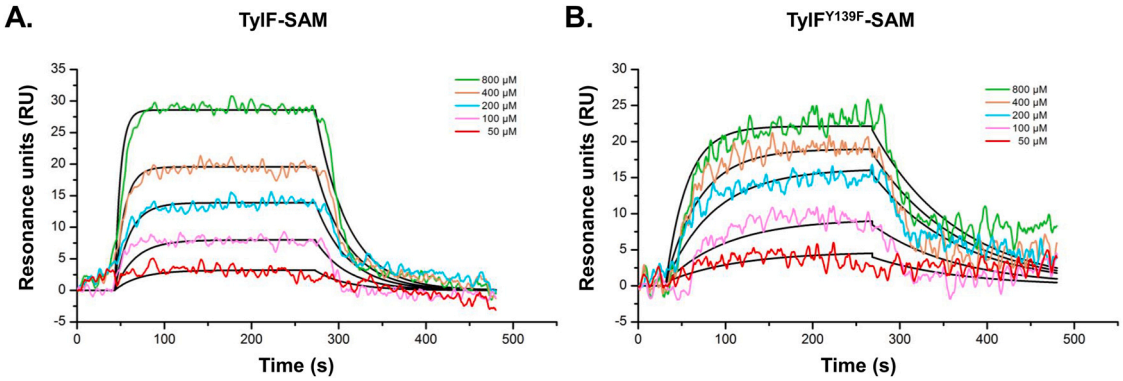

Fig. 6. Binding characteristics analysis between SAM and TylF (TylF^{Y139F}). (A) and (B) The binding affinity was determined using SPR. Sensorgrams showed the binding responses of SAM with TylF and TylF^{Y139F} proteins at different concentrations (50, 100, 200, 400, and 800 μM).

macrocin and tylosin at 30 °C and also remained a more stable high catalytic efficiency in a wide temperature. Therefore, TylF^{Y139F} was considered to be a novel and efficient variant enzyme of TylF. The enzymatic activity depends on its protein structure, and the difference in the relative activity of TylF in vitro may be caused by multiple factors, such as protein structural stability, substrate binding, or substrate exchange. Compared to wild-type protein TylF, TylF^{Y139F} exhibited a greater catalytic efficiency across a wide temperature, suggesting that TylF^{Y139F} has higher protein stability, especially in high temperatures. In addition, binding stability and exchange efficiency of the substrate are also important factors affecting enzyme activity.

Over the past decades, researchers have carried out extensive studies on TylF and its homologous proteins. Two conserved sequences Motif I (rich in glycine) and Motif II (acidic loop) were discovered and thought to be involved in SAM binding, which were widely distributed in TylF *O*-methyltransferase superfamily [37,38]. According to the sequence alignment results, the mutation site of TylF^{Y139F} was not within these two conserved domains. Then, the 3-dimentional structures of proteins TylF and TylF^{Y139F} were predicted using I-TASSER. The results of homology modeling revealed two changed regions (residues 82–86, residues 133–144) and the enlargement of the entrance of adjacent cavity in TylF^{Y139F}. Existing research suggestes that in the TylF *O*-methyltransferase superfamily, such as McyF and NovP, this cavity is where the active site is located, and an N-terminal 'lid loop' (residues 25 −51) and an α-helical 'lid domain' (residues 116 −144) constitute the active site lid [38,39]. Coincidentally, the amino acids 133–143 region of TylF^{Y139F} is located in the 'lid domain'. Because the active site lid of the enzyme forms the access to the cavity and is the gate to the binding pocket, the 'lid domain' would limit substrate (macrocin/tylosin) or cosubstrate (SAM/SAH) exchange, thereby affecting the rate of catalysis. Therefore, it can be speculated that the enlargement of the entrance to the binding pocket caused by the change of the 'lid domain' makes the SAM/SAH or macrocin/tylosin exchange more efficient, which enhances the catalytic activity of TylF^{Y139F}. In addition, another structural change in the amino acids 82–86 region of TylF^{Y139F} happens to be located in the conserved sequence Motif I associated with SAM binding. However, results of binding affinity measurement revealed that the binding of the SAM to the mutant protein TylF^{Y139F} was a little weakened compared with TylF, thus ruling out the possibility that the TylF^{Y139F} could improve catalytic activity by enhancing its binding to the SAM. Thus, it

can be inferred that the disappearance of the α helix in 'lid domain' affects the gate to the binding pocket, and the expansion of the entrance improves the exchange efficiency of substrate or cosubstrate, ultimately enhancing the catalytic activity of the macrocin *O*-methyltransferase TylF^{Y139F}. In summary, the greater protein stability and exchange efficiency of the substrate may be the main reasons for the high catalytic activity of the novel variant TylF^{Y139F}.

5. Conclusions

In this work, we constructed a *tylF* mutant library, and nine mutant strains with improved tylosin production were identified. From these high-yield strains a novel highly efficient methyltransferase variant TylF^{Y139F} was discovered, which provides crucial information for the directed molecular evolution of this important enzyme and further construction of high-yield *S. fradiae* strain for industrial tylosin production.

CRediT authorship contribution statement

Jingyan Fan: Investigation, Methodology, Formal Analysis, Writing – original draft. **Zhiming Yao:** Investigation, Methodology. **Chaoyue Yan:** Investigation, Methodology. **Meilin Hao:** Methodology. **Dai Jun:** Methodology. **Minghui Ni:** Investigation. **Wenjin Zou:** Investigation. **Tingting Li:** Investigation. **Lu Li:** Data curation. **Shuo Li:** Resources. **Jie Liu:** Resources. **Qi Huang:** Data curation, Project administration, Resources, Writing – review & editing. **Rui Zhou:** Conceptualization, Data curation, Funding acquisition, Project administration, Resources, Supervision, Writing – review & editing.

Declaration of Competing Interest

The authors declare that they have no known competing financial interests or personal relationships that could have appeared to influence the work reported in this paper.

Acknowledgments

We thank Hubei Provincial Bioengineering Technology Research Center for Animal Health Products for their technical support. This work was supported by the National Key Research and Development Plans of China (No. 2021YFD1800401 to R. Z.) and the Hubei Provincial Science and Technology Innovation Project (No. 2019AEE005 to R. Z.).

Appendix A. Supporting information

Supplementary data associated with this article can be found in the online version at doi:10.1016/j.csbj.2023.04.005.

References

[1] Hamill RL, Haney Jr. ME, Stamper M, et al. Tylosin, a new antibiotic. II. Isolation, properties, and preparation of desmycosin, a microbiologically active degradation product. Antibiot Chemother 1961;11:328–34.
[2] Gaynor M, Mankin AS. Macrolide antibiotics: binding site, mechanism of action, resistance. Curr Top Med Chem 2003;3(9):949–61.
[3] Arsic B, Barber J, Cikos A, et al. 16-membered macrolide antibiotics: a review. Int J Antimicrob Agents 2018;51(3):283–98.
[4] Debono M, Willard KE, Kirst HA, et al. Synthesis and antimicrobial evaluation of 20-deoxo-20-(3,5-dimethylpiperidin-1-yl)desmycosin (tilmicosin, EL-870) and related cyclic amino derivatives. J Antibiot 1989;42(8):1253–67.
[5] Okamoto R, Fukumoto T, Nomura H, et al. Physico-chemical properties of new acyl derivatives of tylosin produced by microbial transformation. J Antibiot 1980;33(11):1300–8.
[6] Poehlsgaard J, Andersen NM, Warrass R, et al. Visualizing the 16-membered ring macrolides tildipirosin and tilmicosin bound to their ribosomal site. ACS Chem Biol 2012;7(8):1351–5.
[7] Evans NA. Tulathromycin: an overview of a new triamilide antibiotic for livestock respiratory disease. Vet Ther 2005;6(2):83–95.
[8] Zhai H, Luo C, Yang P, et al. Design, synthesis and activity against drug-resistant bacteria evaluation of C-20, C-23 modified 5-O-mycaminosyltylonolide derivatives. Eur J Med Chem 2022;238:114495.
[9] Pape H, Brillinger GU. Metabolic products of microorganisms. 113. Biosynthesis of thymidine diphospho mycarose in a cell-free system from Streptomyces rimosus. Arch Mikrobiol 1973;88(1):25–35.
[10] Jensen AL, Darken MA, Schultz JS, et al. Relomycin: Flask and Tank Fermentation Studies. Antimicrob Agents Chemother (Bethesda) 1963;161:49–53.
[11] Cundliffe E, Bate N, Butler A, et al. The tylosin-biosynthetic genes of Streptomyces fradiae. Antonie Van Leeuwenhoek 2001;79(3–4):229–34.
[12] Baltz RHSE. Genetics of Streptomyces fradiae and tylosin biosynthesis. Annu Rev Microbiol 1988;42:547–74.
[13] Baltz RH, Seno ET. Properties of Streptomyces fradiae mutants blocked in biosynthesis of the macrolide antibiotic tylosin. Antimicrob Agents Chemother 1981;20(2):214–25.
[14] Baltz RH, Seno ET, Stonesifer J, et al. Biosynthesis of the macrolide antibiotic tylosin. A preferred pathway from tylactone to tylosin. J Antibiot 1983;36(2):131–41.
[15] Seno ET, Pieper RL, Huber FM. Terminal stages in the biosynthesis of tylosin. Antimicrob Agents Chemother 1977;11(3):455–61.
[16] Seno ET, Baltz RH. Properties of S-adenosyl-L-methionine:macrocin O-methyltransferase in extracts of Streptomyces fradiae strains which produce normal or elevated levels of tylosin and in mutants blocked in specific O-methylations. Antimicrob Agents Chemother 1981;20(3):370–7.
[17] Seno ET, Baltz RH. S-Adenosyl-L-methionine: macrocin O-methyltransferase activities in a series of Streptomyces fradiae mutants that produce different levels of the macrolide antibiotic tylosin. Antimicrob Agents Chemother 1982;21(5):758–63.
[18] Bauer NJ, Kreuzman AJ, Dotzlaf JE, et al. Purification, characterization, and kinetic mechanism of S-adenosyl-L-methionine:macrocin O-methyltransferase from Streptomyces fradiae. J Biol Chem 1988;263(30):15619–25.
[19] Longwell CK, Labanieh L, Cochran JR. High-throughput screening technologies for enzyme engineering. Curr Opin Biotechnol 2017;48:196–202.
[20] Zeymer C, Hilvert D. Directed evolution of protein catalysts. Annu Rev Biochem 2018;87:131–57.
[21] Cao Y, Li X, Ge J. Enzyme catalyst engineering toward the integration of biocatalysis and chemocatalysis. Trends Biotechnol 2021;39(11):1173–83.
[22] Cadwell RC, Joyce GF. Randomization of genes by PCR mutagenesis. PCR Methods Appl 1992;2(1):28–33.
[23] Stemmer WP. Rapid evolution of a protein in vitro by DNA shuffling. Nature 1994;370(6488):389–91.
[24] Oliphant AR, Nussbaum AL, Struhl K. Cloning of random-sequence oligodeoxynucleotides. Gene 1986;44(2–3):177–83.
[25] Bierman M, Logan R, O'Brien K, et al. Plasmid cloning vectors for the conjugal transfer of DNA from Escherichia coli to Streptomyces spp. Gene 1992;116(1):43–9.
[26] Monk IR, Shah IM, Xu M, et al. Transforming the untransformable: application of direct transformation to manipulate genetically Staphylococcus aureus and Staphylococcus epidermidis. Mbio 2012;3(2).
[27] Hamidian K, Amini M, Samadi N. Consistency evaluation between matrix components ratio and microbiological potency of tylosin major components. Daru 2018;26(2):155–64.
[28] Tan J, Chu J, Hao Y, et al. High-throughput system for screening of Cephalosporin C high-yield strain by 48-deep-well microtiter plates. Appl Biochem Biotechnol 2013;169(5):1683–95.
[29] Li S, Anzai Y, Kinoshita K, et al. Functional analysis of MycE and MycF, two O-methyltransferases involved in the biosynthesis of mycinamicin macrolide antibiotics. Chembiochem 2009;10(8):1297–301.
[30] Kim E, Song MC, Kim MS, et al. Characterization of the Two Methylation Steps Involved in the Biosynthesis of Mycinose in Tylosin. J Nat Prod 2016;79(8):2014–21.
[31] Roy A, Kucukural A, Zhang Y. I-TASSER: a unified platform for automated protein structure and function prediction. Nat Protoc 2010;5(4):725–38.
[32] Yang J, Yan R, Roy A, et al. The I-TASSER Suite: protein structure and function prediction. Nat Methods 2015;12(1):7–8.
[33] Khaliq S, Akhtar K, Afzal Ghauri M, et al. Change in colony morphology and kinetics of tylosin production after UV and gamma irradiation mutagenesis of Streptomyces fradiae NRRL-2702. Microbiol Res 2009;164(4):469–77.
[34] Choi JM, Han SS, Kim HS. Industrial applications of enzyme biocatalysis: current status and future aspects. Biotechnol Adv 2015;33(7):1443–54.
[35] Lin L, Meng X, Liu P, et al. Improved catalytic efficiency of endo-beta-1,4-glucanase from Bacillus subtilis BME-15 by directed evolution. Appl Microbiol Biotechnol 2009;82(4):671–9.
[36] Shao Z, Zhao H, Giver L, et al. Random-priming in vitro recombination: an effective tool for directed evolution. Nucleic Acids Res 1998;26(2):681–3.
[37] Martin JL, McMillan FM. SAM (dependent) I AM: the S-adenosylmethionine-dependent methyltransferase fold. Curr Opin Struct Biol 2002;12(6):783–93.
[38] Gomez Garcia I, Stevenson CE, Uson I, et al. The crystal structure of the novobiocin biosynthetic enzyme NovP: the first representative structure for the TylF O-methyltransferase superfamily. J Mol Biol 2010;395(2):390–407.
[39] Bernard SM, Akey DL, Tripathi A, et al. Structural basis of substrate specificity and regiochemistry in the MycF/TylF family of sugar O-methyltransferases. ACS Chem Biol 2015;10(5):1340–51.